Photoreactivity

DOI: 10.1002/anie.201006057

On the True Photoreactivity Order of {001}, {010}, and {101} Facets of Anatase TiO_2 Crystals**

Jian Pan, Gang Liu, Gao Qing (Max) Lu, and Hui-Ming Cheng**

Design and morphological control of crystal facets is a commonly employed strategy to optimize the performance of various crystalline catalysts from noble metals to semiconductors.[1–8] The basis of this strategy is that surface atomic configuration and coordination, which inherently determine their heterogeneous reactivity, can be finely tuned by morphological control.[3] The conventional understanding of the surface atomic structure of a crystal is that facets with a higher percentage of undercoordinated atoms are usually more reactive in heterogeneous reactions. For instance, {001} facets of anatase TiO_2, which is one of the most important photocatalysts,[9–17] are considered to be more reactive than {101}. We have now discovered, by investigating a set of anatase crystals with predominant {001}, {101}, or {010} facets, that, contrary to conventional understanding, clean {001} exhibits lower reactivity than {101} in photooxidation reactions for OH radical generation and photoreduction reactions for hydrogen evolution. Furthermore, the {010} facets showed the highest photoreactivity. However, these three facets had similar photoreactivity when partially terminated with fluorine. We concluded that a cooperative mechanism of surface atomic structure (the density of undercoordinated Ti atoms) and surface electronic structure (the power of photoexcited charge carriers) is the determining factor for photoreactivity. The findings of this work open up new opportunities for maximizing photoreactivity through morphological control of photocatalysts.

The predicted shape of anatase crystals under equilibrium conditions is a slightly truncated tetragonal bipyramid, enclosed by a majority of {101} and a minority of {001} facets.[18] In contrast to {101} facets with only 50% five-coordinate Ti (Ti_{5c}) atoms, {001} facets with 100% Ti_{5c} atoms were once considered more reactive in heterogeneous reactions.[19–22] A breakthrough by Yang et al. in understanding and controlling crystal facets dramatically increased the ratio of {001} to {101} in anatase, as illustrated in Figure 1 a.[8] Other important low-index facets, namely {010} facets, which also have 100% Ti_{5c} atoms, may be dominant in the elongated truncated tetragonal bipyramids with appropriate surface chemistry, as predicted by Barnard and Curtiss[23] (see the right panel in Figure 1 a), and which was realized recently.[24,25]

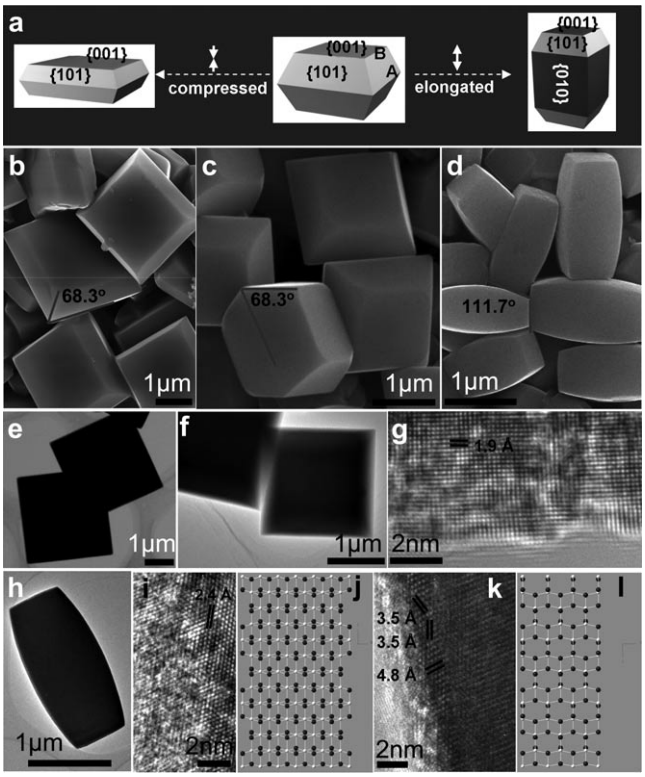

Figure 1. Morphology and atomic structure of anatase TiO_2 crystals. a) Schematic of anatase TiO_2 with different percentages of {101}, {001}, and {010} facets. b–d) SEM images of anatase crystals synthesized with different aqueous solutions of HF (120, 80, and 40 mM) containing different amounts of $TiOSO_4$ precursor (64, 32, and 32 mg) at 180 °C for different times (12, 12, and 2 h). The samples shown in (b–d) are denoted T001-F, T101-F, and T010-F, where T indicates TiO_2, 001/101/010 the dominant facet, and F surface-terminating fluorine. e, f, h) TEM images of representative particles of T001-F, T101-F, and T010-F. g) HRTEM image recorded from typical T001-F particle with [001] orientation. i, k) HRTEM images recorded from another T010-F particle along the $[1\bar{1}0]$ and [010] zone axis. j, l) Projected atomic models along $[1\bar{1}0]$ and [010] directions; white Ti^{4+}, black O^{2-}.

[*] J. Pan, Dr. G. Liu, Prof. H.-M. Cheng
Shenyang National Laboratory for Materials Science
Institute of Metal Research, Chinese Academy of Sciences
72 Wenhua RD, Shenyang 110016 (China)
E-mail: gangliu@imr.ac.cn
cheng@imr.ac.cn
Prof. G. Q. Lu
ARC Centre of Excellence for Functional Nanomaterials
The University of Queensland, Brisbane, Qld. 4072 (Australia)

[**] We thank Dr. C. H. Sun and Dr. Z. G. Chen for their generous help and valuable discussion regarding atomic structure models, Dr. D. M. Tang and Dr. P. F. Yan for their help in TEM characterization, the Major Basic Research Program, Ministry of Science and Technology of China (No. 2009CB220001), NSFC (Nos. 50921004, 51002160, and 21090343), Solar Energy Initiative, and the Funding (KJCX2-YW-H21-01) of the Chinese Academy of Sciences for financial support. GL thanks the IMR SYNL-T.S. Kê Research Fellowship.

Supporting information for this article is available on the WWW under http://dx.doi.org/10.1002/anie.201006057.

The advances in producing low-index facets have broadened the scope for new applications of anatase TiO_2 and make it possible to experimentally investigate the dependence of photoreactivity on the presence of different facets.

The prerequisite for determining the order of facet photoreactivity is to obtain desired clean facets by technically comparable synthesis routes. Recently, anatase crystals with different facets were synthesized by using organic capping surfactants.[24a] However, the facets were heavily coated by organic molecules, making it impossible to study the photoreactivity of different facets. Therefore, it remains a challenging task to prepare anatase with dominant percentages of {001}, {101}, and {010} facets by one synthesis route, and to subsequently evaluate the order of facet photoreactivity.

The key to controlling the percentage of crystallographic facets of anatase crystals is to change the relative stability of each facet during crystal growth, which is intrinsically determined by the surface energies of the facets. Surface-adsorbed fluorine atoms are known to be very effective in changing the surface energy of TiO_2 facets and thus the percentage of facets.[8] Previous results have shown that the percentage of {001} facets of anatase crystals can be increased from 18 up to about 90%, depending on the different synthesis routes.[8,26,27] These results indicate that other facets such as {010}, the surface energy of which ($0.53\ J\,m^{-12}$) is between those of {101} ($0.44\ J\,m^{-12}$) and {001} ($0.90\ J\,m^{-12}$),[18] might also be acquired by fine-tuning the parameters in a given synthesis route so that a favorable surface energy for growing such facets can be obtained. When surface-adsorbed fluorine atoms are used as the morphological controlling agent, clean facets are easily obtained by simple calcination.[8]

Considering the above, we synthesized a set of anatase crystals with different percentages of {001}, {101}, and {010} facets by carefully controlling the synthesis parameters. Representative SEM images of the products are shown in Figure 1b–d (for low-magnification SEM images, see Figure S1, Supporting Information). Their XRD patterns confirm the anatase phase of these crystals (see Figure S2, Supporting Information). According to the symmetries[11] of anatase and a high-resolution (HR) TEM image (Figure 1g), the truncated bipyramids in Figure 1b and c are enclosed by eight isosceles trapezoidal {101} and two square {001} facets. The average particle sizes (the length of A in Figure 1a) and the thicknesses of samples T001-F and T101-F in Figure 1b and c were about 3.1 and 1.8 μm and about 1.1 and 1.6 μm, respectively. The percentages of {001} and {101} facets of T001-F and T101-F are given in Table 1.

Compared to the shape of the truncated bipyramid in Figure 1b,c, Figure 1d shows that an additional quartet column is generated at the center of a particle, so that the truncated bipyramid is separated into two parts located at the ends of the column. The shape of these particles is consistent with the predicted morphology enclosed by {001}, {101}, and {010} facets of anatase.[23] The angle of $(111.7 \pm 0.4)°$ between the top square and the lateral trapezoid in Figure 1d corresponds to the obtuse angle between the {001} and {101} facets. The HRTEM image in Figure 1i recorded along the $[1\bar{1}0]$ zone axis of a single T010-F anatase crystal shows the {004} lattice fringes with a spacing of 2.4 Å. Figure 1k, recorded along the [001] direction, shows three sets of lattice fringes with spacings of 3.5, 3.5, and 4.8 Å, corresponding to {101}, $\{10\bar{1}\}$, and {002} facets, respectively. These atomic structures, revealed by the HRTEM images, are consistent with the projected structure models of an ideal particle enclosed by {001}, {101}, and {010} facets along the [001] and $[1\bar{1}0]$ directions as shown in Figure 1j,l. Clearly, these well-faceted particles (denoted T010-F) in Figure 1d can be easily identified as having {001}, {101}, and {010} facets according to the SEM and TEM images, as well as the crystallographic symmetries of anatase. The average length of particles is about 1.7 μm and the percentage of each type of facets is summarized in Table 1.

Table 1: Average percentages of {001}, {101}, and {010} facets in T001-F, T101-F, and T010-F, calculated from the surface area of each facet from SEM images.

Sample	{001}	{101}	{010}
T001-F	40%	60%	0%
T101-F	24%	76%	0%
T010-F	14%	33%	53%

The different facets of anatase particles given in Table 1 allow us to investigate their respective photocatalytic activities. The photooxidation and photoreduction activities of the synthesized anatase samples were estimated by evaluating the amount of OH radicals generated by reported methods[28] and the rate of hydrogen evolution from the photoreduction reaction. All three samples (T001-F, T101-F, and T010-F) with fluorine-terminated surfaces show very similar abilities for generating OH radicals (Figure 2a). Their hydrogen-evolution rates are also nearly identical (Figure 2b). After removing the surface fluorine atoms of T001-F, T101-F, and T010-F, the corresponding fluorine-free samples, denoted T001, T101, and T010, showed apparently improved photooxidation and photoreduction capabilities (Figure 2a and b). Furthermore, the new photoreactivity order is T010 > T101 > T001 in the photooxidation and reduction reactions for generating OH radicals and hydrogen evolution, respectively. Therefore, we can draw the conclusion that clean {001}, {101}, and {010} facets follow the photoreactivity order of {001} < {101} < {010}, while the facets partially terminated with fluorine have similar photoreactivity. This is contrary to the conventional understanding that the photoreactivity of {001} is greater than that of {101}.

Although a difference in particle size and specific surface area (ranging from 1 to $2\ m^2 g^{-1}$) exists among the above samples, the results in Figure 2 clearly indicate that the surface fluorine termination and the percentages of different crystal facets are two determining factors in controlling the photoreactivity of anatase. Apparently, surface fluorine termination can completely counteract the effect of different facets on photoreactivity. This can be explained by the role of fluorine termination in changing surface Ti_{5c} atoms to Ti_{6c}, which greatly impairs surface reactivity,[19] and consequently modifies the force constants of the surface Ti-O-Ti network imposed by the presence of surface Ti–F bonds. The chemical state of fluorine as Ti–F species is evidenced by the F 1s X-ray

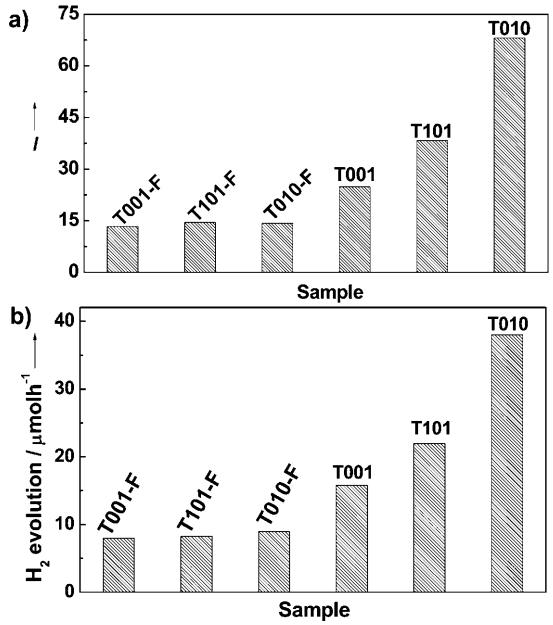

Figure 2. Photoreactivity comparison. a) Fluorescence signal intensity of TAOH at 426 nm and b) hydrogen evolution rate from water containing 10 vol% methanol for surface fluorine-terminated anatase TiO_2 crystals T001-F, T101-F, and T010-F and clean anatase TiO_2 crystals T001, T101, and T010. All samples for measurements of hydrogen evolution were deposited with 1 wt% Pt cocatalyst.

photoelectron spectrum (Figure 3a), which shows a binding energy of 684.1 eV in all three samples.[8] The amount of fluorine in T001-F, T101-F, and T010-F is 4.8, 4.3, and 4.9 atom%, respectively. No sulfur species was detected. The modified force constants are clearly revealed by comparing the Raman spectra of fluorine-terminated TiO_2 with normal anatase (Figure 3b). Two features are evident: 1) shifting of the E_g mode at 144 cm^{-1} to higher frequency, and 2) weakening of the B_{1g} mode at 397 cm^{-1}. Therefore, we concluded that the apparent change in surface structure imposed by the presence of surface Ti–F bonds is the reason for the reactivity order of {001}-F ≈ {101}-F ≈ {010}-F.

After removing the surface fluorine (see Figure S3, Supporting Information) from T001-F, T101-F, and T010-F, Figure 3c demonstrates that the chemical states of elemental Ti and O in T001, T101, and T010 (Ti $2p_{3/2}$ binding energy 458.5 eV; O 1s binding energy 529.7 eV) are identical. Furthermore, the Raman spectra in Figure 3d show that the effects of active mode shifting of E_g and weakening of B_{1g} caused by the Ti–F bonds are fully eliminated. It suggests that the surface structures of crystal facets {101}, {001}, and {010} have been almost completely recovered, so that the photoreactivity of different facets with exposed undercoordinated Ti atoms on the surface is superior to their fluorine-terminated counterparts.

The commonly used criteria to predict the photoreactivity of crystal facets is the density of surface undercoordinated atoms.[19,20] Figure 4a shows the atomic structural model of {101}, {001}, and {010} facets. With 100% unsaturated Ti_{5c} atoms at the surface, {001} facets are theoretically considered more reactive than {101} with 50% Ti_{5c} atoms and 50% Ti_{6c} atoms in heterogeneous reactions.[19,20] However, as revealed in Figure 2, {001} has lower photoreactivity than {101}, contrary to the prediction, while {010}, which also has 100% Ti_{5c} atoms exposed, gives the highest photoreactivity among

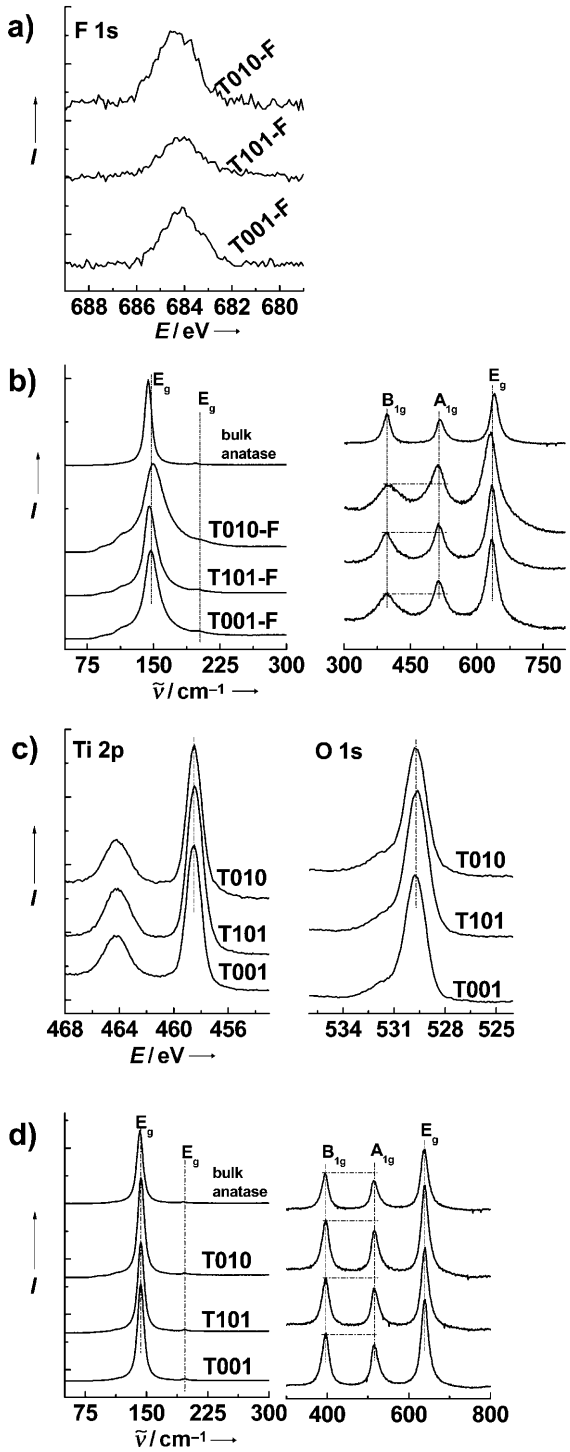

Figure 3. X-ray photoelectron and Raman spectra. a) F 1s XP spectra of T001-F, T101-F, and T010-F. b) Raman spectra of T001-F, T101-F, T010-F and reference bulk anatase. c) Ti 2p and O 1s XP spectra of T001, T101, and T010. d) Raman spectra of T001, T101, T010 and reference bulk anatase TiO_2.

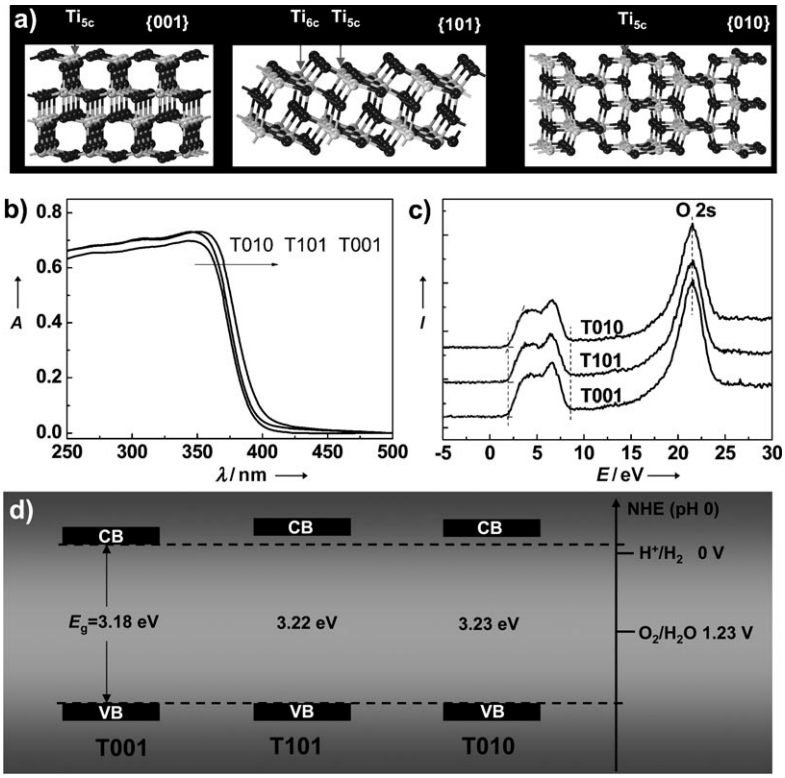

Figure 4. Surface atomic structure and electronic structure. a) Schematic of atomic structure of {101}, {001}, and {010} faces. b) UV/Vis absorption spectra of T001, T101, and T010. c) Valence-band XP spectra of T001, T101, and T010. d) Determined valence-band and conduction-band edges of T001, T101, and T010.

the three facets. The question then arises what is the underlying factor that reverses the predicted photoreactivity order of {101} and {001} facets, and why do {010} facets give the highest photoreactivity?

The process of photocatalysis with semiconductor photocatalysts involves three mechanistic steps: excitation, bulk diffusion, and surface transfer of photoexcited charge carriers.[29,30] The photocatalytic reactivity can therefore be simultaneously tuned through the synergistic effects of absorbance, redox potential, and mobility of charge carriers, which are determined by electronic band structures, in addition to their surface atomic structure. Consequently, the photoreactivity of a crystal facet must be related to both its surface atomic structure and surface electronic band structure.

Electronic band structures of the anatase crystals with different crystal facets were investigated (Figure 4b–d). UV/Vis absorption spectra (Figure 4b) demonstrate that, although T001, T101, and T010 have comparable absorbance, the absorption edge of T001 has a redshift of about 6 nm with respect to those of T101 and T010. Previous results confirmed that the {001} facet has a smaller bandgap than the {101} facet due to different atomic configurations.[26] Therefore, the higher percentage of {001} in T001 is responsible for this redshift. The absorption edge of T101 and T010 with dominant {101} and {010} facets nearly overlap, that is, {010} and {101} facets have very close bandgaps. It is therefore clearly determined that the bandgaps of facets discussed here satisfy the order $\{101\} \approx \{010\} > \{001\}$. X-ray photoelectron valence-band (VB) spectra (Figure 4c) reveal that VB maxima of all three TiO_2 crystals are at 1.93 eV, that is, the conduction-band (CB) minimum of T101 and T010 is raised in contrast to T001. Furthermore, the nearly identical widths of their valence bands of about 6.74 eV indicate similar mobilities of charge carriers. The resolved band structures of different crystals are illustrated in Figure 4d. The absence of reduction states and upward shift of VB maxima in our measured VB spectra are attributed to the negligible amount of oxygen vacancies in our TiO_2 samples, in contrast to the typically reduced TiO_2 single crystals used in surface-science studies.[11] The existence of oxygen vacancies can substantially shift the VB maximum downwards as a result of band-blending effects and introduce defect states of Ti^{3+} in the band gap.[11,31]

Now we can address the true determining factors of the photoreactivity order of the {001}, {101}, and {010} facets by considering the cooperative effects of surface atomic coordination and band structure. In terms of surface Ti_{5c} atoms, both {001} and {010} would exhibit a higher photoreactivity than {101}. Conversely, {101} and {010} should have superior photoreactivity to {001} when considering that more strongly reductive electrons can be generated on {101} and {010} facets with a higher CB minimum. Apparently, {010} facets have both a favorable surface atomic structure and a surface electronic structure, so that the more strongly reducing electrons in the CB can be transferred via the surface Ti_{5c} atoms as active reaction sites. The efficient consumption of excited electrons in the photoreduction reactions can simultaneously promote the involvement of holes in photooxidation reactions. Such a cooperative mechanism existing on {010} facets is responsible for its having the highest reactivity.

Finally, it is useful to discuss the possible influence of surface reconstruction on photocatalytic activity of different facets. Selloni and coauthors discussed the 1×4 reconstruction on {001} in terms of the "ad-molecule" (ADM) model,[32] in which rows of bridging oxygen atoms are replaced with rows of TiO_3 species forming a chain. As a result, additional more unsaturated Ti_{4c} atoms are formed on {001} surface besides the original Ti_{5c} atoms. On the other hand, Diebold et al. demonstrated that the $1 \times n$ reconstruction on {100} will introduce a surface with {101} microfaceted grooves running in the [010] direction.[33,34] Consequently, the density of unsaturated Ti atoms on reconstructed {100} will be lower than that on an ideal {100} face. Based on the conventional understanding of surface structure that facets with a higher percentage of undercoordinated atoms are usually more reactive in heterogeneous reactions, reconstructed {001} should have had higher photocatalytic activity than reconstructed {100}. However, as demonstrated in this work, this hypothesis is not supported. Therefore, the proposed coop-

erative mechanism of surface structure and electronic structure still works well even when possible reconstruction is considered.

Experimental Section

Sample synthesis: 64, 32, and 32 mg of titanium oxysulfate ($TiOSO_4 \cdot x H_2O$, FW: 159.9 g mol^{-1}) powder was dissolved in aqueous solutions of HF with concentrations of 120, 80, and 40 mM, respectively, to prepare the $TiOSO_4$ aqueous solution precursor for anatase TiO_2 crystals T001-F, T101-F, and T010-F. In the typical synthesis routes for samples T001-F, T101-F, and T010-F, 40 mL of the $TiOSO_4$ solution were transferred to a Teflon-lined autoclave and heated at 180 °C for 12, 12, and 2 h, respectively. After reaction, the products were collected by centrifugation and washed with deionized water several times to remove dissolvable ionic impurities. The samples were then dried at 80 °C in air for 12 h.

Surface-fluorine removal from as-prepared anatase TiO_2: Powder samples of the as-prepared anatase TiO_2 crystals were heated at 600 °C in a static air atmosphere in a furnace for 2 h. The samples were then allowed to cool to room temperature.

Cocatalyst loading: Pt loading was conducted by an impregnation method in an aqueous solution of $H_2PtCl_6 \cdot 6H_2O$. A sample of TiO_2 was added to an aqueous solution containing the desired amount of $H_2PtCl_6 \cdot 6H_2O$ (1 mg mL^{-1} Pt) in an evaporating dish at 60 °C. The suspension was evaporated under constant stirring, and the resulting powder was collected and heated in air at 180 °C.

Characterization: X-ray diffraction patterns of the samples were recorded on a Rigaku diffractometer with Cu radiation. Their morphology was determined by transmission electron microscopy (TEM) on a Tecnai F30. The BET surface area was determined by nitrogen adsorption/desorption isotherm measurements at 77 K (ASAP 2010). Chemical compositions and valence-band spectra of TiO_2 were analyzed by X-ray photoelectron spectroscopy (Thermo Escalab 250, monochromatic $Al_{K\alpha}$ X-ray source). All binding energies were referenced to the C 1s peak (284.6 eV) arising from adventitious carbon. The optical absorbance spectra of the samples were recorded in a UV/Vis spectrophotometer (JACSCO-550). The fluorescence emission spectrum was recorded at room temperature with excitation by incident light of 325 nm wavelength with a fluorescence spectrophotometer (Hitachi, F-4500). Raman spectra were collected with LabRam HR 800.

Photoreactivity measurements: Photocatalytic hydrogen evolution reactions were carried out in a top-irradiation vessel connected to a glass-enclosed gas circulation system. 100 mg of the photocatalyst powder were dispersed in 300 mL aqueous solution containing 10 vol% methanol. The reaction temperature was maintained below 9 °C. The amount of H_2 evolved was determined by using a gas chromatograph (Agilent Technologies: 6890N).

OH radical reactions were performed as follows: 5 mg of photocatalyst were suspended in 80 mL aqueous solution containing 0.01 M NaOH and 3 mM terephthalic acid. Before exposure to light, the suspension was stirred in the dark for 30 min. Five milliliters of the solution were then taken out after irradiation for 25 min and centrifuged for fluorescence spectroscopy measurements. During the photoreactions, no oxygen bubbled into the suspension. A fluorescence spectrophotometer was used to measure the fluorescence signal of the 2-hydroxy terephthalic acid generated. The excitation light used in recording fluorescence spectra was 320 nm.

The light source in the above photoreactivity experiments was a 300 W Xe lamp (Beijing Trusttech Co. Ltd, PLS-SXE-300UV).

Received: September 28, 2010
Revised: November 1, 2010
Published online: January 26, 2011

Keywords: crystal growth · heterogeneous catalysis · hydrothermal synthesis · photochemistry · titania

[1] X. G. Peng, L. Manna, W. D. Yang, J. Wickham, E. Scher, A. Kadavanich, A. P. Alivisatos, *Nature* **2000**, *404*, 59.
[2] Y. G. Sun, Y. N. Xia, *Science* **2002**, *298*, 2176.
[3] N. Tian, Z. Y. Zhou, S. G. Sun, Y. Ding, Z. L. Wang, *Science* **2007**, *316*, 732.
[4] B. Lim, M. J. Jiang, P. H. C. Camargo, E. C. Cho, J. Tao, X. M. Lu, Y. M. Zhu, Y. N. Xia, *Science* **2009**, *324*, 1302.
[5] X. W. Xie, Y. Li, Z. Q. Liu, M. Haruta, W. J. Shen, *Nature* **2009**, *458*, 746.
[6] M. Law, L. E. Greene, J. C. Johnson, R. Saykally, P. D. Yang, *Nat. Mater.* **2005**, *4*, 455.
[7] H. Q. Yan, R. R. He, J. Pham, P. D. Yang, *Adv. Mater.* **2003**, *15*, 402.
[8] H. G. Yang, C. H. Sun, S. Z. Qiao, J. Zou, G. Liu, S. C. Smith, H. M. Cheng, G. Q. Lu, *Nature* **2008**, *453*, 638.
[9] A. Fujishima, K. Honda, *Nature* **1972**, *238*, 37.
[10] R. Asahi, T. Morikawa, T. Ohwaki, K. Aoki, Y. Taga, *Science* **2001**, *293*, 269.
[11] U. Diebold, *Surf. Sci. Rep.* **2003**, *48*, 53.
[12] B. O'Regan, M. Grätzel, *Nature* **1991**, *353*, 737.
[13] M. Grätzel, *Nature* **2001**, *414*, 338.
[14] E. L. Crepaldi, G. J. D. A. Soler-Illia, D. Grosso, F. Cagnol, F. Ribot, C. Sanchez, *J. Am. Chem. Soc.* **2003**, *125*, 9770.
[15] P. Prene, E. Lancelle-Beltran, C. Boscher, P. Belleville, P. Buvat, C. Sanchez, *Adv. Mater.* **2006**, *18*, 2579.
[16] H. Tada, T. Mitsui, T. Kiyonaga, T. Akita, K. Tanaka, *Nat. Mater.* **2006**, *5*, 782.
[17] H. Tada, T. Kiyonaga, S. Naya, *Chem. Soc. Rev.* **2009**, *38*, 1849.
[18] M. Lazzeri, A. Vittadini, A. Selloni, *Phys. Rev. B* **2001**, *63*, 155409.
[19] A. Selloni, *Nat. Mater.* **2008**, *7*, 613.
[20] X. Q. Gong, A. Selloni, *J. Phys. Chem. B* **2005**, *109*, 19560.
[21] A. Vittadini, A. Selloni, F. P. Rotzinger, M. Gratzel, *Phys. Rev. Lett.* **1998**, *81*, 2954.
[22] Y. W. Jun, M. F. Casula, J. H. Sim, S. Y. Kim, J. Cheon, A. P. Alivisatos, *J. Am. Chem. Soc.* **2003**, *125*, 15981.
[23] A. S. Barnard, L. A. Curtiss, *Nano Lett.* **2005**, *5*, 1261.
[24] a) C. T. Dinh, T. D. Nguyen, F. Kleitz, T. O. Do, *ACS Nano* **2009**, *3*, 3737; b) B. H. Wu, C. Y. Guo, N. F. Zheng, Z. X. Xie, G. D. Stucky, *J. Am. Chem. Soc.* **2008**, *130*, 17563.
[25] J. M. Li, D. S. Xu, *Chem. Commun.* **2010**, *46*, 2301.
[26] G. Liu, C. H. Sun, H. G. Yang, S. C. Smith, L. Z. Wang, G. Q. Lu, H. M. Cheng, *Chem. Commun.* **2010**, *46*, 755.
[27] X. Han, Q. Kuang, M. Jin, Z. Xie, L. Zheng, *J. Am. Chem. Soc.* **2009**, *131*, 3152.
[28] T. Hirakawa, Y. Nosaka, *Langmuir* **2002**, *18*, 3247.
[29] M. R. Hoffmann, S. T. Martin, W. Choi, D. W. Bahnemann, *Chem. Rev.* **1995**, *95*, 69.
[30] A. L. Linsebigler, G. Q. Lu, J. T. Yates, Jr., *Chem. Rev.* **1995**, *95*, 735.
[31] J. B. Simonsen, B. Handke, Z. S. Li, P. J. Møller, *Surf. Sci.* **2009**, *603*, 1270.
[32] M. Lazzeri, A. Selloni, *Phys. Rev. Lett.* **2001**, *87*, 266105.
[33] N. Ruzycki, G. S. Herman, L. A. Boatner, U. Diebold, *Surf. Sci.* **2003**, *529*, L239.
[34] U. Diebold, N. Ruzycki, G. S. Herman, A. Selloni, *Catal. Today* **2003**, *85*, 93.

